JARO 13: 447–459 (2012)
DOI: 10.1007/s10162-012-0320-9

JARO
Journal of the Association for Research in Otolaryngology

Reverse Transmission along the Ossicular Chain in Gerbil

Wei Dong[1], Willem F. Decraemer[2], and Elizabeth S. Olson[1]
[1]*Department of Otolaryngology, Head and Neck Surgery, Columbia University, 630 West 168th Street, New York, NY 10032, USA*
[2]*University of Antwerp, CGB, Groenenborgerlaan 171, 2020 Antwerpen, Belgium*

Received: 31 August 2011; Accepted: 11 March 2012; Online publication: 31 March 2012

ABSTRACT

In a healthy cochlea stimulated with two tones f_1 and f_2, combination tones are generated by the cochlea's active process and its associated nonlinearity. These distortion tones travel "in reverse" through the middle ear. They can be detected with a sensitive microphone in the ear canal (EC) and are known as distortion product otoacoustic emissions. Comparisons of ossicular velocity and EC pressure responses at distortion product frequencies allowed us to evaluate the middle ear transmission in the reverse direction along the ossicular chain. In the current study, the gerbil ear was stimulated with two equal-intensity tones with fixed f_2/f_1 ratio of 1.05 or 1.25. The middle ear ossicles were accessed through an opening of the pars flaccida, and their motion was measured in the direction in line with the stapes piston-like motion using a laser interferometer. When referencing the ossicular motion to EC pressure, an additional amplitude loss was found in reverse transmission compared to the gain in forward transmission, similar to previous findings relating intracochlear and EC pressure. In contrast, sound transmission along the ossicular chain was quite similar in forward and reverse directions. The difference in middle ear transmission in forward and reverse directions is most likely due to the different load impedances—the cochlea in forward transmission and the EC in reverse transmission.

Keywords: middle ear, ossicles, middle ear gain, otoacoustic emissions

Correspondence to: Wei Dong · Department of Otolaryngology, Head and Neck Surgery · Columbia University · 630 West 168th Street, New York, NY 10032, USA. Telephone: +1-212-3053993; fax: +1-212-3052249; email: wd2015@columbia.edu

INTRODUCTION AND BACKGROUND

Since Kemp's (1978) discovery of otoacoustic emissions (OAEs), OAEs have been used for probing the active process of the cochlea. The middle ear is responsible for transmitting sound in and out of the cochlea, thus it shapes the OAE as well as the primaries. Consequently, it is important to understand how the middle ear transmits sound reversely, from the cochlea to the ear canal (EC). In forward sound transmission, the external and middle ear convey environmental sound to the inner ear, the cochlea. The middle ear plays the role of an impedance matcher, coupling the relatively low acoustic impedance of the EC to the much higher input impedance of the cochlea. Sound pressure drives the tympanic membrane (TM), which induces vibration along the ossicular chain, composed of the malleus, incus, and stapes. The stapes vibration produces an intracochlear pressure that is larger than the input pressure at the TM, which is characterized as "middle-ear pressure gain." This pressure gain through the middle ear has been studied in cat (Decory et al. 1990; Nedzelnitsky 1980), chinchilla (Decory et al. 1990; Slama et al. 2010), gerbil (de La Rochefoucauld et al. 2008; Dong and Olson 2006; Olson 1998, 2001), guinea pig (Dancer and Franke 1980; Decory et al. 1990; Magnan et al. 1997), and human temporal bone (Aibara et al. 2001; Nakejima et al. 2008; Puria 2003a; Puria et al. 1997). In addition to the pressure gain, the more recent studies also document a delay associated with the transmission between the EC and cochlea.

The effect of the middle ear on OAEs has been explored in live humans with EC pressure measurements (Keefe 2002; Keefe and Abdala 2007). In animals and human temporal bones, intracochlear pressure near the stapes can be measured, thus

forward and reverse transmission can be evaluated directly. For example, using two-tone distortion products (DPs) as the intracochlear sound source and simultaneously measuring responses in the EC and at the stapes, reverse transmission through the middle ear has been explored in cat (Voss and Shera 2004), gerbil (Dong and Olson 2006), and guinea pig (Magnan et al. 1997). In a study with human temporal bones (Puria 2003a), an intracochlear sound source was used to drive the middle ear reversely, and forward and reverse transmission were quantified. All of these studies showed gain and delay in forward transmission (from the EC to the stapes or scala vestibuli (SV) close to the stapes) and loss and delay in backward transmission (from the stapes or SV to the EC). In related work, Dalhoff et al. (2011) compared DPs on the umbo and EC for diagnosis of hearing problems. Our previous results comparing forward and reverse transmission in gerbil provided background to the present study, with an example shown in Figure 1. The forward transfer function (FTF), defined as P_{SV}/P_{EC} at the primary frequencies, had a relatively flat amplitude ratio across frequencies corresponding to a gain of ~25 dB (red and green in Fig. 1A). The phase difference between P_{SV} and P_{EC} (red and green in Fig. 1B) varied nearly linearly with frequency indicating a constant delay that was estimated as ~32 μs by visually fitting a straight line (dotted in Fig. 1B) to the phase versus frequency curve. The reverse transfer function (RTF), defined as P_{EC}/P_{SV} at DP frequencies (blue and cyan in Fig. 1A), approximately followed the trend of the FTF from 8 to 22 kHz but with a RTF loss that was 10 to 20 dB larger than the FTF gain. Thus, the RTF was not a simple inverse of the FTF because in that case, when plotted in decibels, FTF and −RTF would overlie each other. The reverse delay, estimated from the phase versus frequency curve (blue and cyan in Fig. 1B), was ~38 μs, slightly longer than the FTF delay.

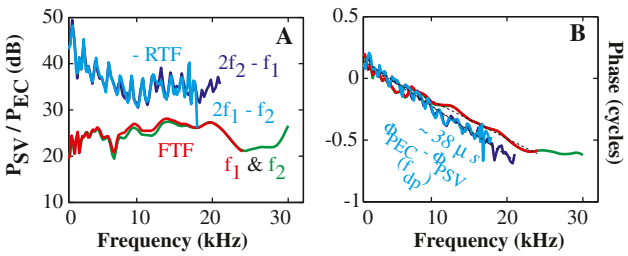

FIG. 1. Previous measurements of middle ear forward (FTF) and reverse transfer function (RTF) evaluated via simultaneous measurements of P_{EC} and P_{SV} close to the stapes (adapted from Dong and Olson 2006, Fig. 5). **A** FTF, defined as P_{SV}/P_{EC} at primary frequencies, and RTF, defined as P_{EC}/P_{SV} at DP frequencies. **B** P_{SV} phase referenced to P_{EC}. *Red*, *green*, *cyan*, and *blue* represent components of f_1, f_2, $2f_1–f_2$, and $2f_2–f_1$, respectively. ($L_1=L_2=90$ dB SPL, $f_2/f_1=1.25$, wg67. The bulla was open, and the sound was delivered in a closed-field configuration).

In the current study, we take a more detailed look to determine the basis for the difference between forward and reverse transmission. One strong possibility is that the TM does not work as well as a sound source as it does as a sound collector (Puria et al. 1993, 2003a, b). Another possible contributor to the difference is that the ossicles do not move in an efficient manner in reverse transmission: The cochlear load is much larger than the EC load, and the stapes is constrained in the annular ligament, thus in reverse transmission, the ossicles might move in a looser and less effective manner than in forward transmission.

The gerbil ear was stimulated with two equal-intensity tones with fixed f_2/f_1 ratio over a wide frequency range. A family of stimulus parameter-dependent DPs is generated in healthy gerbil cochleae (e.g., Dong and Olson 2005). The intracochlear DP pressure drives the stapes and produces vibrations along the ossicular chain, which drive TM motion, producing distortion product otoacoustic emissions (DPOAEs) in the EC. Simultaneous EC pressure and velocity measurements were made on ossicles along an axis nearly in line with the stapes piston-like motion direction through an opening of pars flaccida (PF). The primary objective of the study was to compare forward (at primary frequencies) and reverse transmission (at DP frequencies) along the ossicular chain in order to see if forward/reverse differences in ossicular motion were contributing to our previous results, in which there was extra pressure loss in the RTF compared to the FTF.

EXPERIMENTAL DESIGN AND METHODS

Experiments were performed in deeply anesthetized young adult female gerbils 40–60 g in mass. Fourteen gerbils were used in this study. The care and use of the animals were approved by the Institutional Animal Care and Use Committee of Columbia University. Ketamine (40 mg/kg) was administered first to sedate the animal. Sodium pentobarbital (initial dose 60 mg/kg, supplemental 10 mg/kg) was used for maintenance of anesthesia, and the analgesic buprenorphine (20 mg/kg) was administered every 6 h. At the end of the experiment, the animal was sacrificed with an overdose of sodium pentobarbital. During the experiment, animal core temperature was maintained at ~37°C using a thermostatically controlled heating blanket. A tracheotomy was performed to maintain a patent airway. The left pinna was removed. The bulla was vented by a long thin silicone tube (5–6 cm long with an inner diameter of 0.28 mm) to avoid static pressure buildup in the bulla cavity. In this configuration, the bulla was acoustically closed because only

very low frequencies will equilibrate. A buildup of static pressure is easy to identify because the PF is then visibly distorted. In order to access the middle ear ossicles along the stapes' piston-like motion direction, the PF was removed in later measurements, which provides a much larger vent (Fig. 2), and its effects are described below.

The experimental strategy was to apply two-tone acoustic stimulation and make simultaneous measurements of EC pressure and ossicular motion. The primary responses were used to measure forward transmission and the DPs and DPOAEs to measure reverse transmission. (Note: we denote by "DP" the motion at distortion product frequencies measured on the ossicles and by "DPOAE" the distortion product otoacoustic emission pressure in the EC.) Stimulus and acquisition programs were written in Matlab and the TDT Visual Design Studio. The sampling frequency of the TDT system was 200 kHz. Two equal-intensity tones (1–2 s duration) with fixed f_2/f_1=1.05 or 1.25 were generated by a Tucker Davis Technology (TDT) system III. Data were stored following removal of the first 4,096 points of the response waveform to avoid the transient, and time-averaging the remaining waveform, typically in 50 time-locked segments. Responses were later analyzed by Fourier transform in Matlab. The primary frequencies were swept from 1 to 50 kHz in 500-Hz steps.

A Bruel and Kjaer probe-tube microphone (model 4134) served as the EC pressure monitor. The transfer function of the probe-tube microphone was accounted for when setting the sound pressure level (SPL, decibels relative to 20 μPa peak) and analyzing the data. With a 1-s data acquisition time, the microphone noise level (with probe-tube) was ~5 to 10 dB SPL up to 30 kHz.

Velocities (V) at points along the ossicular chain and on the TM were sequentially measured using a Laser-Doppler vibrometer (LDV, Polytec, OFV-534, and VD-06 decoder). The vibrometer's Helium–Neon laser was focused on the preparation with a 10× Mitutoyo lens with 33.5 mm focusing distance. As reported by the manufacturer, the focused spot size ($1/e^2$) is 3 μm. The noise level of the velocity measurement depends on the amount of reflected light and was typically less than 10^{-4} mm/s at frequencies below 30 kHz and somewhat larger at higher frequencies. Reflective glass beads (MO-SCI Corp, 5–25 μm) with a thin coating of gold (50 nm gold evaporated in the lab) were hand-deposited with a fine pin on the TM and middle ear ossicles to improve the optical signal. The beads did not affect the motion of the ossicular system; motions were similar with and without the beads. The mass of the bead was at most 4×10 g, which is much smaller than the mass of any ossicle.

The measuring direction was approximately perpendicular to the stapes footplate; this is the direction of the piston-like motion of the stapes. The velocity of the manubrium and TM could be measured with an intact TM; however, measuring responses from the malleus and incus required removal of the PF. Therefore, in the early stage of each experiment, measurements were made from the lateral process of the malleus (LPM), the manubrium, and the TM before removing the PF. Then, more measurements were made along the ossicular chain and on the TM

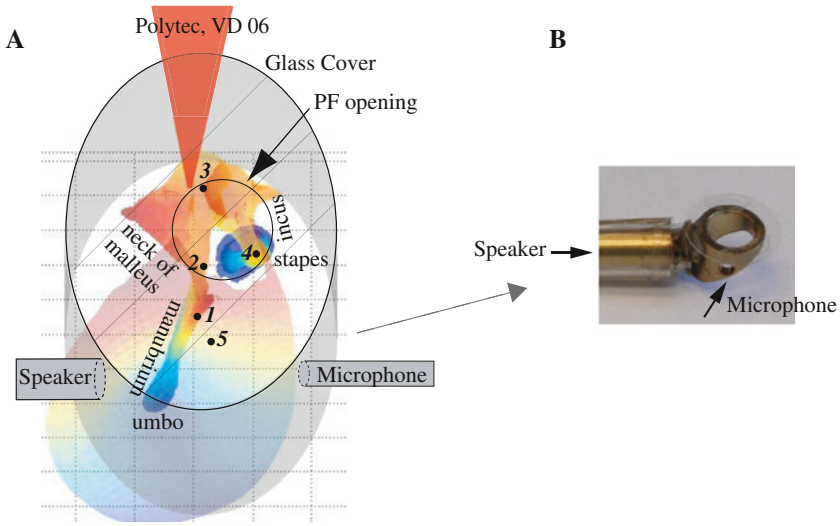

FIG. 2. Experimental access with closed-field sound configuration. **A** Illustration of the experimental access with closed-field sound configuration. P_{EC} was measured at the EC opening entrance with a Bruel and Kjaer probe-tube microphone, and simultaneously, velocity was measured along the ossicular chain by a laser vibrometer. The recorded points are *1*=lateral process of the malleus (*LPM*); *location between 2 and 3*=neck of malleus (*NM*); *3*=malleus–incus joint (either on malleus or incus; *MI joint*); *location between 3 and 4*=incus; *4*=long process of incus (*LPI*); *5*=point on tympanic membrane (*TM*). **B** Brass fixture with glass window that was coupled to the EC opening during closed-field sound experiments.

with PF removed. The measurement locations are marked with black dots in Figure 2: LPM, neck of the malleus (NM), malleus-incus joint (MI-joint) either on malleus or incus, incus, long process of incus (LPI), and TM. The velocity was also measured somewhat lower on the manubrium (about one third of the manubrium length down from the LPM) and umbo in a few cases. From the PF opening indicated in Figure 2, it is seen that measurements on the LPM, manubrium, and TM were made at an angle to the piston-like direction. Because our goal is to compare forward and reverse transmission, no correction for the viewing angle was needed or performed.

With equal intensity and f_2/f_1 ratio of 1.05, the DPOAEs $2f_1-f_2$ and $2f_2-f_1$ were similar to each other in size and extended up to 25 to 30 kHz in a healthy gerbil ear. With f_2/f_1 ratio of 1.25, the $2f_1-f_2$ DPOAE was usually larger than with the 1.05 ratio; however, the frequency range over which it could be detected was smaller. In order to evaluate middle ear reverse transmission over a wide frequency range, we used two f_2/f_1 ratios (1.05 and 1.25) and the highest possible primary sound pressure level for which there was no system distortion contamination. Two different acoustic configurations were used: In 2008, we used an open-field sound configuration with Walkman earphone (Sony) coupled to the Bruel and Kjaer probe-tube microphone, which was positioned ~1–2 cm away from the EC opening. In order to produce a robust DP signal, the primary tones were delivered at 85–90 dB SPL. In 2009, a brass fixture with glass window was fashioned to fit over the EC opening so that we could observe the ossicular motion in a closed-field sound configuration (Fig. 2). In this case, we used an electrostatic sound driver. With the brass fixture, the position of the microphone's probe-tube was better controlled at ~6–7 mm away from the LPM, and the primary tones were delivered at 80 dB SPL. The level of distortion products produced by the system (mainly the driver) has been discussed previously (Dong and Olson 2006, 2008). With the 2008 system, system distortion was at least 60 dB smaller than the 90-dB SPL primaries, and with the 2009 system, the distortion was ~70 dB smaller than the 80-dB SPL primaries. At these levels, system distortion was not a concern in the results. System distortion was also checked with postmortem responses at the end of each experiment.

The acoustic load at the EC was different in the open- and closed-cavity configurations. Based on past work, we expected the differences in results due to the different loads to be small. For example, in our own studies, small ripples in the RTF seemed to be related to the tube connecting the sound source in a closed configuration (Dong and Olson 2006). Withnell et al. (1998) compared open- and closed-field electrically evoked emissions in guinea pig and found that the emissions were the same above 5 kHz, and below 5 kHz, the open-field emissions were smaller. However, other studies in the literature observed larger load-dependent effects on emissions (Nakajima et al. 1994; Puria et al. 1997). Thus, the degree of load-dependent variation depends on the loads being compared. In the present study, there were some differences in the results of the two types of load, but they did not influence our primary results. The results presented here are labeled "date–month–year" with open- and closed-field in 2008 and in 2009, respectively.

Most of the results are comparisons of forward and reverse transmission functions, which we abbreviated as FTF and RTF. For example, when considering incus velocity and EC pressure, the |FTF| is $|V_{LPI}|/|P_{EC}|$ at f_1 or f_2, and the |RTF| is $|P_{EC}|/|V_{LPI}|$ at f_{dp}. The magnitude plots compare |FTF| to 1/|RTF|. If reverse transmission were a simple inverse of forward transmission, |FTF| and 1/|RTF| would overlie each other in the plot. The FTF phase in this example is $\Phi_{forward}=\Phi_{VLPI}-\Phi_{PEC}$, at f_1 and f_2, and the RTF phase is $\Phi_{reverse}=\Phi_{PEC}-\Phi_{VLPI}$, at f_{dp}. Group delays are calculated as the slope of straight-line fits of $\Phi_{forward}$ and $\Phi_{reverse}$ versus frequency. Similar FTF and RTF functions were defined at the other observation locations.

RESULTS

In ten of the 14 animals used, the cochleae were maintained in healthy condition so that DPs and DPOAEs could be recorded. Results are presented from those animals. The results were similar across animals (three with open-field and seven with closed-field sound configuration). The $2f_1-f_2$ and $2f_2-f_1$ DPs are typically largest and were used in presenting the results. A single measurement run gives the information needed to find both forward and reverse transmission between the given velocity measurement point and the EC pressure; thus, a time-related change in cochlear condition will not affect our comparison of forward and reverse middle ear transmission.

Effect of pars flaccida removal

The LPM is a location on the ossicles that abuts the PF and thus can be accessed before and after the removal of the PF (Fig. 2). Therefore, it was used to evaluate changes due to PF removal. The velocity measurement at the LPM was also repeated after a few hours to confirm repeatability (not shown). The effects of PF removal on the amplitude (Fig. 3A) and phase (Fig. 3B) of $FTF_{EC\text{-}LPM}$ and $RTF_{EC\text{-}LPM}$ were determined by making velocity measurements from a bead on the LPM (Fig. 2) before and after opening the PF

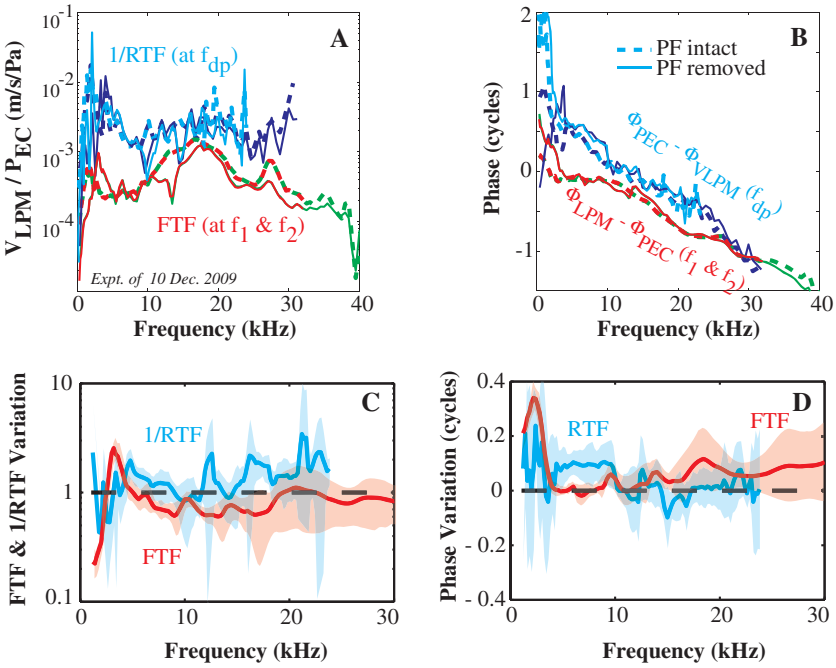

FIG. 3. Effect of PF removal. The responses measured at the LPM before and after opening PF. An individual example is in **A** and **B** (experiment: 10 Dec. 2009, $L_1=L_2=80$ dB, $f_2/f_1=1.25$, closed field). **A** Amplitude: V_{LPM}/P_{EC}. **B** Phase: $V_{LPM}-P_{EC}$ at f_1 and f_2; $P_{EC}-V_{LPM}$ at f_{dp}. *Dotted thick and solid thin lines* indicate the results with PF intact and removed, respectively. *Red* and *green* are responses at f_1 and f_2 frequencies; *cyan* and *blue* are responses at $2f_1-f_2$ and $2f_2-f_1$ frequencies. **C**, **D** The average change in FTF and 1/RTF upon PF removal, using five data sets like that in **A** and **B**. **C** Amplitude change (after/before). **D** Phase difference (after–before). *Bold* and *shaded* indicate average±standard deviation.

in an individual animal. This control measurement was made in five experiments in 2009 (experiments: 15 Dec. 2009, 10 Dec. 2009, 9 Dec. 2009, 4 Dec. 2009, and 2 Dec. 2009) with similar results. The average variation upon PF removal of $FTF_{EC\text{-}LPM}$ and $RTF_{EC\text{-}LPM}$ is in panels C and D. The bulla was vented as described in "Experimental design and methods" section, and the sound was delivered to the EC in the closed-field configuration illustrated in Figure 2.

Consistent with previous studies (de La Rochefoucauld et al. 2008, 2010; Teoh et al. 1997), in the FTF, removing the PF caused substantial change only at low frequencies (red and green curves in Fig. 3A, B). Changes in $RTF_{EC\text{-}LPM}$ were small in both amplitude and phase at frequencies above 2 kHz (blue and cyan in Fig. 3A, B). At frequencies above 4 kHz, the average amplitude ratio (after/before removal of the PF) was close to 1 (Fig. 3C), and the maximum average phase variation was less than 0.1 cycles (Fig. 3D). Thus, we conclude that at frequencies above 4 kHz, normal middle ear function in forward and reverse transmission can be studied with PF removed. Therefore, the results at frequencies above 4 kHz are emphasized.

Forward and reverse transfer function between ear canal and lateral process of the malleus

Beyond demonstrating the effects of PF removal, Figure 3A, B illustrate $FTF_{EC\text{-}LPM}$ and $RTF_{EC\text{-}LPM}$ between the EC and LPM. Grouped results of the transfer function between EC and LPM are in Figure 4A–D, with open- and closed-field results grouped separately. Average±standard deviations are plotted along with an individual case (dotted), which helps for understanding the variability. The closed- and open-field cases show the same trends reported for the single case shown in Figure 3A, B.

$1/RTF_{EC\text{-}LPM}$ was larger than the $FTF_{EC\text{-}LPM}$ (Fig. 3A). The $FTF_{EC\text{-}LPM}$ delay found with a straight line fit to the phase curve (Fig. 3B) was ~46 μs. The acoustic delay corresponding to the 6-mm distance between the probe-tube and the TM corresponds to an acoustic delay of 18 μs. Thus, the FTF delay is 46–18=28 μs. The $RTF_{EC\text{-}LPM}$ delay was similar but slightly longer (slightly steeper line) in agreement with the previous results relating P_{SV} at the stapes to EC pressure (Fig. 1). At frequencies below 10 kHz, the $RTF_{EC\text{-}LPM}$ phase curve sloped up very steeply, much more than the $FTF_{EC\text{-}LPM}$ phase curve (Fig. 3B). This sudden increase in slope of the ossicular motion phase was not seen in the results of Figure 1. Because frequencies less than 7 kHz are affected by open versus closed bulla (de La Rochefoucauld et al. 2010) and the bulla was open for the Figure 1 measurements, this difference might be due to methodological differences. Except for this difference, the major forward versus reverse transmission differences seen from the previous study relating P_{SV} to EC pressure (Fig. 1) were also present when relating LPM velocity to EC pressure: 10 to 20 dB more loss in reverse transmission than gain in forward transmission (Figs. 3A and 4A, C), and a few microseconds longer delay in reverse transmission (Figs. 3B and 4B, D).

Forward and reverse transfer function between ear canal and long process of the incus

Stapes velocity (V_{stapes}) is often used as a measure of the middle ear output to the cochlea (Decraemer et

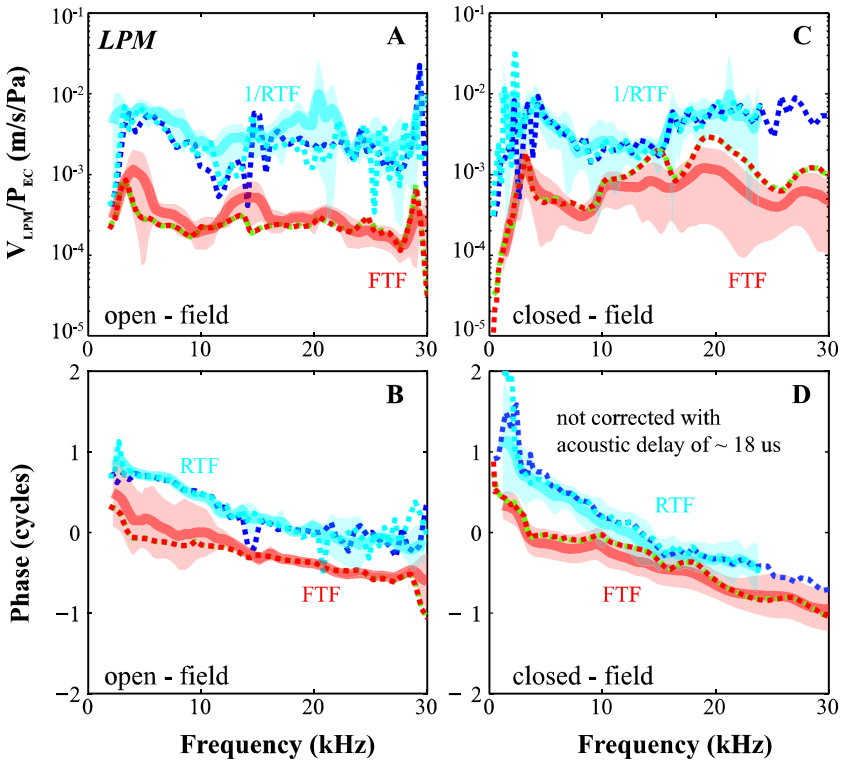

FIG. 4. $FTF_{EC\text{-}LPM}$ and $RTF_{EC\text{-}LPM}$ with open- and closed-field sound configuration. Amplitude (**A**, **C**) and phase (**B**, **D**) of $FTF_{EC\text{-}LPM}$ and $RTF_{EC\text{-}LPM}$ with open- and closed-field sound configuration averaged across two and six animals, respectively. *Bold* and *shaded* indicate average±standard deviation of f_1 and f_2 for FTF (*red*) and $2f_1–f_2$ and $2f_2–f_1$ for RTF (*cyan*). *Dotted lines* represent individual responses with open (10 Apr. 2008) and closed field (15 Dec. 2009). *Green*, *red*, *cyan*, and *blue* stand for f_2, f_1, $2f_1–f_2$, and $2f_2–f_1$. $|1/RTF_{EC\text{-}LPM}|$ was ~10–20 dB larger than $|FTF_{EC\text{-}LPM}|$. The group delay estimated by fitting a *straight line* with the phase–frequency curves showed a slightly longer $RTF_{EC\text{-}LPM}$ delay than $FTF_{EC\text{-}LPM}$ delay.

al. 2007; Ravicz et al. 2008). In a recent study, the LPI and the head of the stapes moved very similarly in gerbil in forward sound transmission, indicating that there was very little slippage at the incudostapedial joint in the piston-like direction (de La Rochefoucauld et al. 2008). In a few cases in the present study, the velocities of the LPI and the head of the stapes were measured with two-tone stimulation along the stapes piston-like direction, and there was little difference either at primary or DP frequencies. This suggested that there is also little slippage across this incudostapedial joint in the reverse direction. Therefore, V_{LPI} at primary and DP frequencies were considered as a measure of middle ear input to and from the cochlea, in order to find $FTF_{EC\text{-}LPI}$ and $RTF_{EC\text{-}LPI}$.

Figure 5 plots the averaged results of $FTF_{EC\text{-}LPI}$ and $RTF_{EC\text{-}LPI}$ calculated from the simultaneous measurements of P_{EC} and V_{LPI} with open- (three animals) and closed-field sound configurations (five animals), respectively. Examples from individual animals are also plotted in dotted lines to indicate variability. The average $FTF_{EC\text{-}LPI}$ (V_{LPI}/P_{EC} at f_1 and f_2) was around 10^{-4} m/s/Pa from 4 to 30 kHz (red in Fig. 5A, C). The shape of $1/RTF_{EC\text{-}LPI}$ (average V_{LPI}/P_{EC} at $2f_1–f_2$ and $2f_2–f_1$; cyan in Fig. 5A, C) was similar to the $FTF_{EC\text{-}LPI}$ from 4 to 25 kHz, but it was displaced upward almost 20 dB, indicating ~20 dB more loss for reverse transmission than gain for forward transmission. The phase of the $RTF_{EC\text{-}LPI}$ was steeper than the $FTF_{EC\text{-}LPI}$.

These observations are similar to the previous results when P_{SV} was compared to P_{EC}, shown in Figure 1 (Dong and Olson 2006) in that (1) the magnitude of $1/RTF_{EC\text{-}LPI}$ was substantially larger than $FTF_{EC\text{-}LPI}$, and (2) the reverse delay was slightly longer than the forward delay. The similarity in forward/reverse differences in P_{SV}/P_{EC} and V_{LPI}/P_{EC} argues that the basis for the forward/reverse difference is lateral to the stapes.

Relative motion along the ossicular chain

To explore the motion along the ossicular chain in more detail, Figure 6 compares forward and reverse transmission at the LPM and LPI. The velocity ratio and phase difference of V_{LPM} and V_{LPI} are presented in two groups corresponding to open- (Fig. 6A, B) and closed-field sound configurations (Fig. 6C, D). Responses of two individual cases are in thin solid

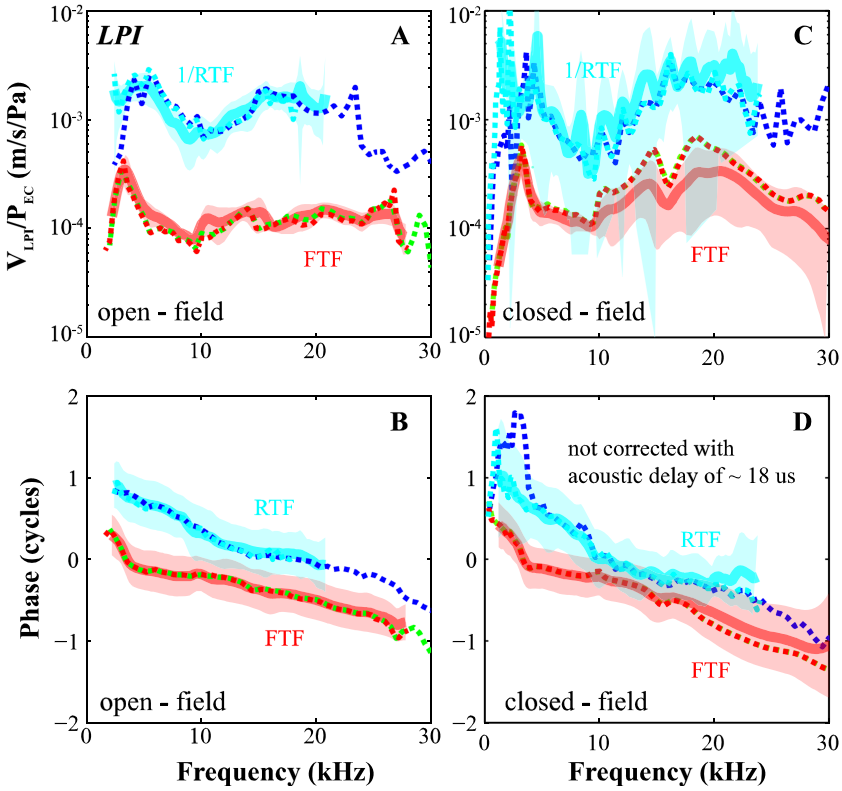

FIG. 5. $FTF_{EC\text{-}LPI}$ and $RTF_{EC\text{-}LPI}$ with open- and closed-field sound configuration. Amplitude (**A**, **C**) and phase (**B**, **D**) of $FTF_{EC\text{-}LPI}$ and $RTF_{EC\text{-}LPI}$ with open- and closed-field sound configuration averaged across three and five animals, respectively. *Bold* and *shaded* indicate average±standard deviation of f_1 and f_2 for $FTF_{EC\text{-}LPI}$ (*red*) and $2f_1–f_2$ and $2f_2–f_1$ for $RTF_{EC\text{-}LPI}$ (*cyan*). *Dotted lines* represent individual responses with open (10 Apr. 2008) and closed field (15 Dec. 2009). *Green*, *red*, *cyan*, and *blue* stand for f_2, f_1, $2f_1–f_2$, and $2f_2–f_1$, respectively.

and thin dashed lines to give an indication of variability. The average of the two responses is plotted with thick lines.

The average velocity amplitude ratio shows that with the view through the open PF, the LPM velocity was ~2.5–4 times larger than LPI velocity in forward transmission (red in Fig. 6A, C). This held for both open and closed configurations. In reverse transmission, the velocity ratio was similar to forward, except for a dip to a value of 1–2 between ~11 and 18 kHz that occurred in both open and closed configurations (cyan in Fig. 6A, C). The phase differences in forward transmission were small, less than 0.2 cycles up to 30 kHz, and erratic, but the overall trend indicated that from LPM to LPI, there was a transmission delay of ~8 μs (Fig. 6B, D). The reverse transmission delay was similar to the forward delay up to ~14 kHz and was slightly more erratic above 14 kHz.

To explore the forward:reverse comparison further, in Figure 7, displacement results are shown from a single preparation (experiment: 15 Dec. 2009), in which measurements were made at the four locations

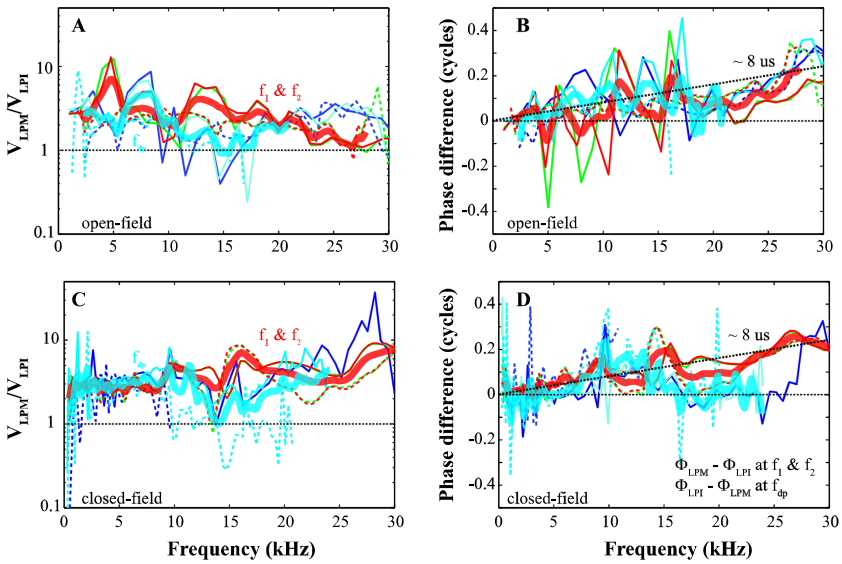

FIG. 6. Relative velocity and phase between LPM and LPI. **A**, **C** Velocity ratio V_{LPM}/V_{LPI}. **B**, **D** Phase difference between V_{LPM} and V_{LPI} for open- and closed-field sound configuration. f_1, f_2, $2f_1–f_2$, and $2f_2–f_1$ are *green*, *red*, *cyan*, and *blue*, respectively. *Thin solid and dotted lines* were responses of two individual animals. *Thick lines* indicate the average at primary (*red*) or DP frequencies (*cyan*). All responses were at least 10 dB above the noise.

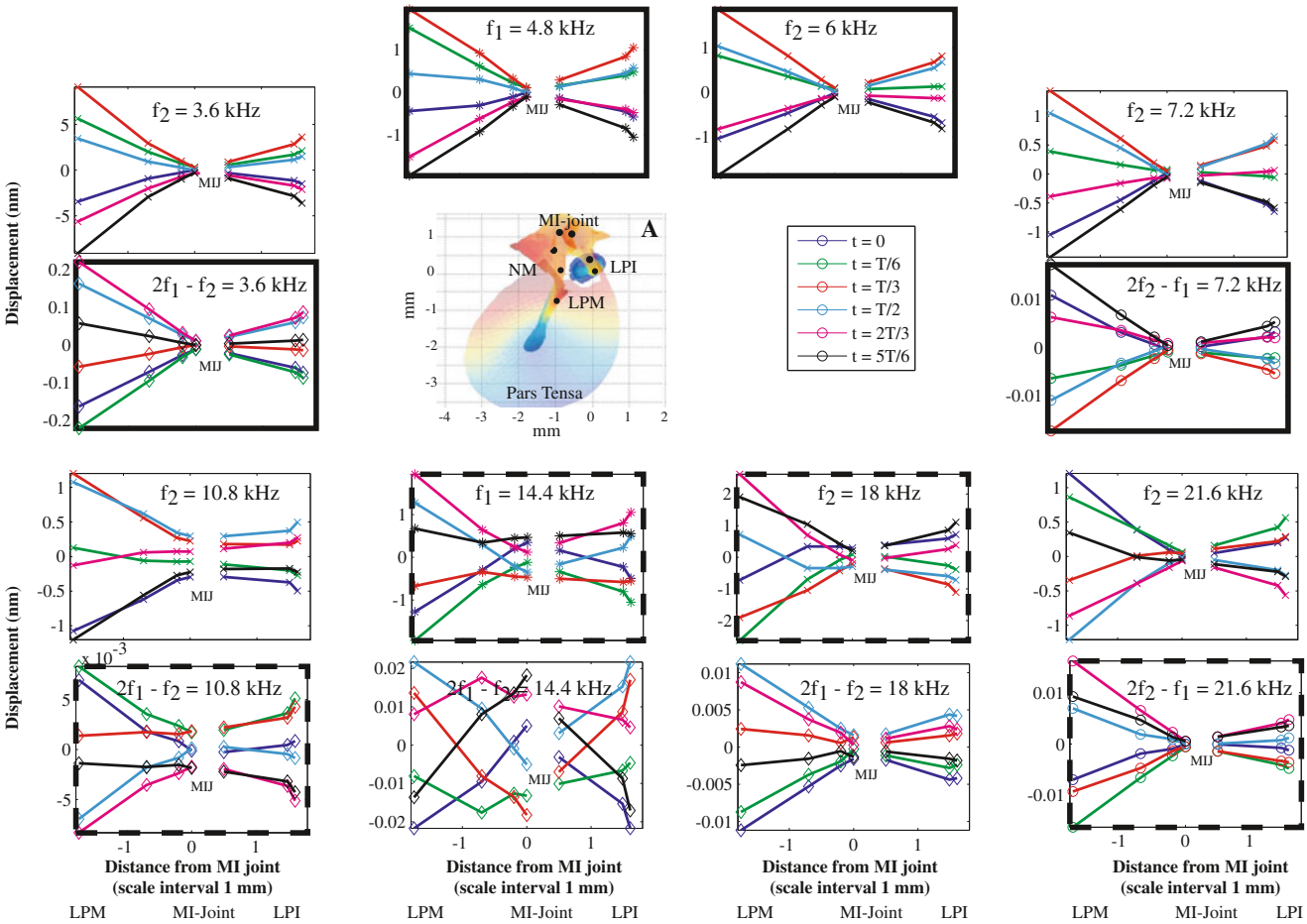

FIG. 7. Displacement along the ossicular chain. **A** Recording locations along the ossicular chain. The other panels show displacements along the ossicular chain at six equally spaced instants of time during the cycle. The displacements at the observation points are shown as a function of their distance to the MI joint. Data for the malleus are shown at the *left*, data for the incus at the *right*. The *bold solid frames* show a data set with f_1 and f_2=4.8 and 6 kHz, and the *bold dashed frame* show data with f_1 and f_2=14.4 and 18 kHz. To compare forward and reverse transmission at several frequencies, DPs and primaries are paired in the frames that partner with the bold frames. (Experiment: 15 Dec. 2009, L_1=L_2=80 dB, f_2/f_1=1.25).

on the malleus and the three locations on the incus indicated in panel A. The data are plotted at one frequency in each panel, with approximate distance at the observation point to the MI-joint on the *x*-axis. The point locations were estimated by correlating photos taken during the experiment to a 3D reconstructed gerbil middle ear model (Decraemer et al. 2007). The *y*-axis shows the displacement, positive towards the viewer (vibrometer). Displacements at six equally spaced instants of time in the cycle (0, T/6, 2T/6...5T/6 in blue, green, red, cyan, magenta, and black) are shown, resulting in a stroboscopic animation of the motion of the observation points. The starting phase was not set to be the same at the different frequencies. The bold solid frames show data that were collected with a single set of two-tone stimulation with f_1 and f_2 frequencies of 4.8 and 6 kHz. The bold dashed frames show data collected from a single set of two-tone stimulation with f_1 and f_2 frequencies of 14.4 and 18 kHz. Each of these bold outlined sets illustrates the simultaneous motion of the ossicles in forward and reverse transmission. Thus, considering the solid bold set, one can think of these different motions being superimposed in time—as the f_1 and f_2 travel inward, the $2f_1-f_2$ and $2f_2-f_1$ travel outward simultaneously. The same can be said for the dashed bold set.

The panels are also presented in pairs of results in which a primary frequency is matched with a similar DP frequency. By considering the two panels in a pair, one can compare forward and reverse transmission at a given frequency—this comparison is more critical to the overall topic of this paper, which is to compare forward and reverse transmission. The frequencies range was from 3.6 to 21.6 kHz. From this frequency-by-frequency comparison, there are two main observations: (1) Motion along the chain at primary and DP frequencies is very similar in forward and reverse transmission at five frequencies (3.6, 7.2, 10.8, 18, and 21.6 kHz), but the motions differ at 14.4 kHz. (The

start phase is generally different in the different panels, and we are concerned with the overall motion patterns.) (2) At the lower frequencies of 3.6 and 7.2 kHz, the motion of the point close to the MI-joint is very small compared to that of the LPM and the LPI. At 21.6 kHz, this is again observed. At 10.8 and 18 kHz and the forward transmission case at 14.4 kHz, the motion of the point close to the MI-joint is less than of the LPM and LPI but not by so much. At 14.4 kHz, the motion in reverse transmission is almost as large at the MI-joint as at the LPM and LPI, and the motion looks erratic. From the figure here, except for 14.4 kHz, the motion along the ossicular chain appears very similar for forward and reverse transmission at any given frequency. This is consistent with the grouped results plotted in Figure 6, where except at frequencies around ~11–18 kHz, forward and reverse transmission were very similar.

During the experiment, the measurement locations were chosen for good reflectivity and not for co-linearity. In order to study the mode of vibration, co-linearity is of great advantage because it allows one to decide whether a body behaves rigidly or not. If the resulting interpolation along co-linear points is a straight line, then the measured motion is consistent with rigid body motion. In Figure 8, the results of Figure 7 were interpolated at co-linear points, using the Matlab interpolation script TriScatteredInterp. The interpolated motion was found separately for the incus and malleus. The real and imaginary part of the velocity response was interpolated, rather than amplitude and phase, to avoid phase unwrapping difficulties.

In Figure 8, the interpolated results are shown at eight frequencies. For the displacements of forward transmission (indicated with circles and solid lines), we used data from the primary frequency f_1, and for the displacements of reverse transmission (crosses and dashed lines), we used data obtained at $2f_1-f_2$. In order to facilitate comparison of forward and reverse motion, for reverse transmission, we scaled the displacements of each ossicle by a constant factor and shifted the displacement of each ossicle by a constant phase so that the amplitude and phase of the vibration for the signal going in the reverse direction would be similar to the vibration signal propagating in

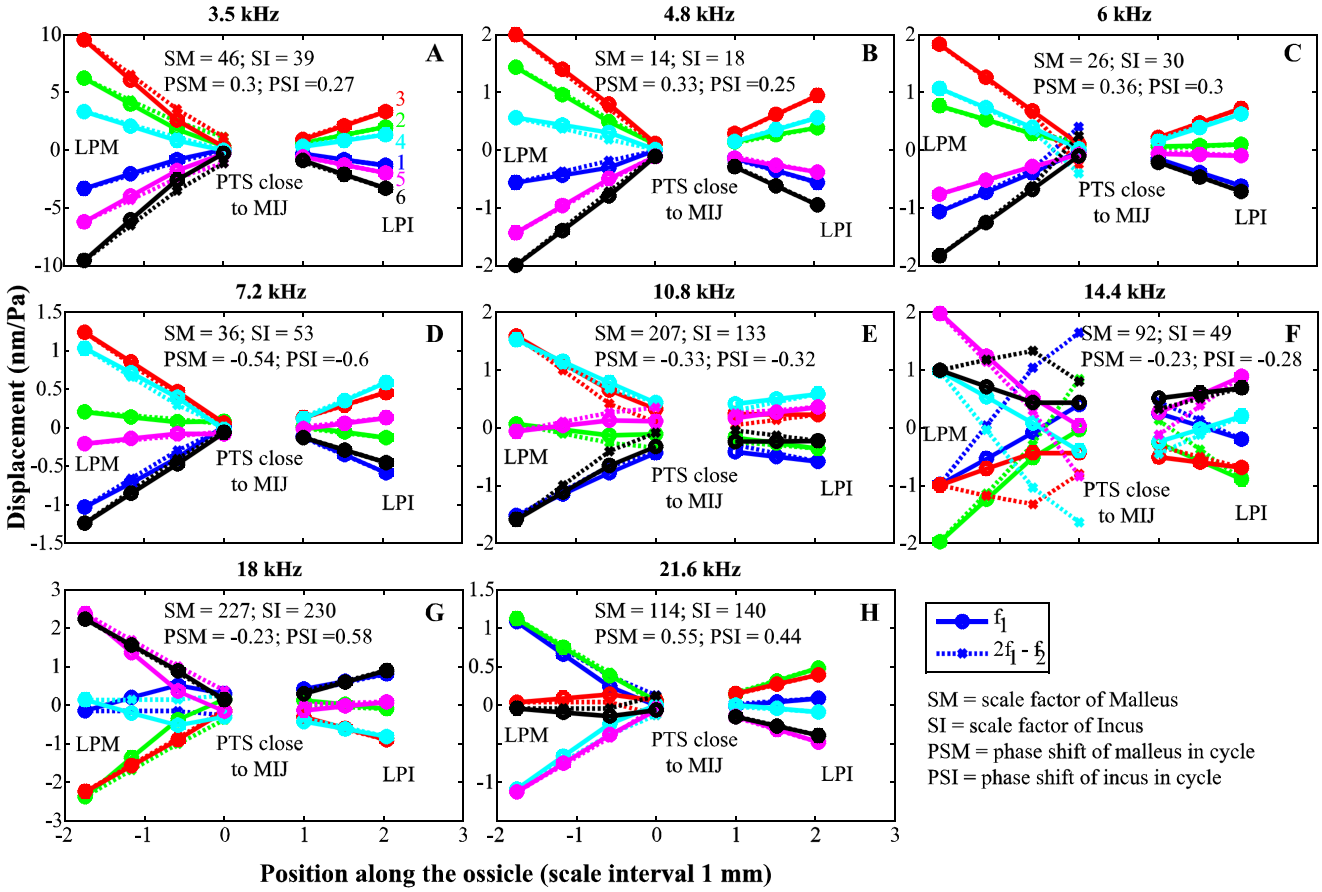

FIG. 8. Displacement along ossicular chain from LPM to LPI in a co-linear system. This figure is comparable to the displacement panels of Figure 7, but now the displacement in forward and reverse transmission are shown in the same panel. The reverse displacements were scaled and shifted in time (see annotation in each panel). *Different colors* indicate different times in a cycle. *Solid and dotted lines* represent f_1 and $2f_1-f_2$ in forward and reverse transmission, respectively.

the forward direction at the LPM for the malleus and LPI for the incus, respectively. This scale and phase shift was done separately for the malleus and the incus. The scale factor and phase shift (in cycle) are annotated in each panel. Thus, relative timing between incus and malleus cannot be visualized in this figure—to give a specific example, the red curve on the incus occurred at a different time in the cycle than the red curve on the malleus. The relative timing can be deduced using the annotated phase shifts or by consulting Figure 7, where there were no phase shifts applied.

Considering the motion at a given frequency in a given panel, it is striking that the mode of vibration of the malleus and incus is so similar in forward (f_1) and in reverse ($2f_1–f_2$). Even at 14.4 kHz (Fig. 8F), in which the agreement is far from exact, the evolution of the displacement with time in the cycle is still the same. The similar vibration mode is observed in the low frequency panels (3.5, 4.8, 6, and 7.2 kHz) and also at the highest frequency of 21.6 kHz; the malleus displacement gradually decreases from LPM to MI-joint (for the malleus interpret MI-joint as "on the malleus close to the MI-joint"), and the incus displacement increases from the MI-joint ("on the incus close to the MI-joint") to the LPI. For both malleus and incus, the displacements become very small at the MI-joint. This indicates that the mode of vibration is mainly a rotation about an axis in the region of the MI-joint. (Note that with a single observation direction and collinear observation points, we can only probe the rotation component about an axis perpendicular to the observation points.) At 10.8 kHz, the mode has changed somewhat, and at 14.4 kHz, the mode of vibration cannot be described as a rotation. A vibration mode similar to that at 14.4 kHz only occurred at frequencies between 14 and 15 kHz. At higher frequencies (18 and 21.6 kHz), the mode is again dominated by rotation.

For the incus, we had only three measured points, and with just three data points, the interpolated motion appears rigid by default: the 2D interpolation is done on the surface defined by the original data points, and this surface is a plane surface when only three points are available. On the malleus, four data points were used for the interpolation, and in this case, some deviation from straight motion is apparent in the Figure 8 results, but not much—the motion is largely consistent with rigid body motion, allowing for a small experimental error of a few percent. Even at 14.4 kHz, the erratic appearance of the motion is for the most part due to the wobbling of the anatomical rotation axis during the cycle. Nevertheless, in our past work on forward transmission, where observations at more points on the malleus and the incus (six or more) were made, the motion of the gerbil malleus and incus was quite rigid up to at least 20 kHz, with a small amount of non-rigidity beyond (Decraemer et al. 2011). In reverse transmission, the interpolated motion plots in Figure 8 are somewhat less straight, likely in part due to a larger experimental uncertainty given the substantially smaller vibration amplitudes. Overall, these results point to rigid body behavior, and we intend to look further into this question in both forward and reverse transmission in future work.

Along manubrium, from lateral process of the malleus to close to the umbo

Up to this point, forward and reverse transmission have been shown to be similar from the LPM to the LPI, thus the difference in forward and reverse transmission is predominantly lateral to the LPM—between the LPM and the EC. This includes the motion of the manubrium and TM and radiation of sound out from the manubrium and TM to the EC. This mechano-acoustical coupling was not explored in detail in the present study, but in Figure 9, we include one more data set, in which measurements were made on the manubrium close to the umbo (~1 mm), as shown in Figure 9D (experiment: 8 Apr. 2008, open-field). In Figure 9A, velocity is plotted relative to the EC pressure, as FTF and 1/RTF. V_{LPI}, V_{LPM}, and V_{umbo} are shown with thin, dashed, and thick lines, respectively. Phase referenced to P_{EC} is in Figure 9B. Velocity ratios, plotted with respect to V_{LPI}, are in Figure 9C.

In forward transmission, velocities of the LPM and the location close to the umbo were similar to each other and ~2–4 times bigger than V_{LPI} (Fig. 9A, C). (In a previous study, the center of the umbo moved ~twice as much as the LPM in forward transmission (de La Rochefoucauld and Olson 2010), and the LPI and LPM motions were more similar. The difference in the present study is likely due to the angle of approach of the current measurements, which was relatively less perpendicular to the manubrium—in the previous study, the EC was enlarged for a relatively perpendicular approach.) In reverse, V_{LPM}/V_{LPI} was similar to that shown in Figure 6A and was similar to the ratio in forward transmission. The most interesting finding is that in the reverse but not the forward direction, the location close to the umbo moved with a much greater velocity than the LPM from 8 to 16 kHz (Fig. 9A, C), which is a substantial departure from the forward:reverse similarity along the ossicles documented up to this point. V_{umbo}/V_{LPI} at f_{dp} peaked at 10 kHz, where the umbo velocity was ~12 times greater than that of V_{LPI}.

The phase of umbo, LPM, and LPI velocity showed a systematic accumulation with frequency both in forward and in reverse transmission.

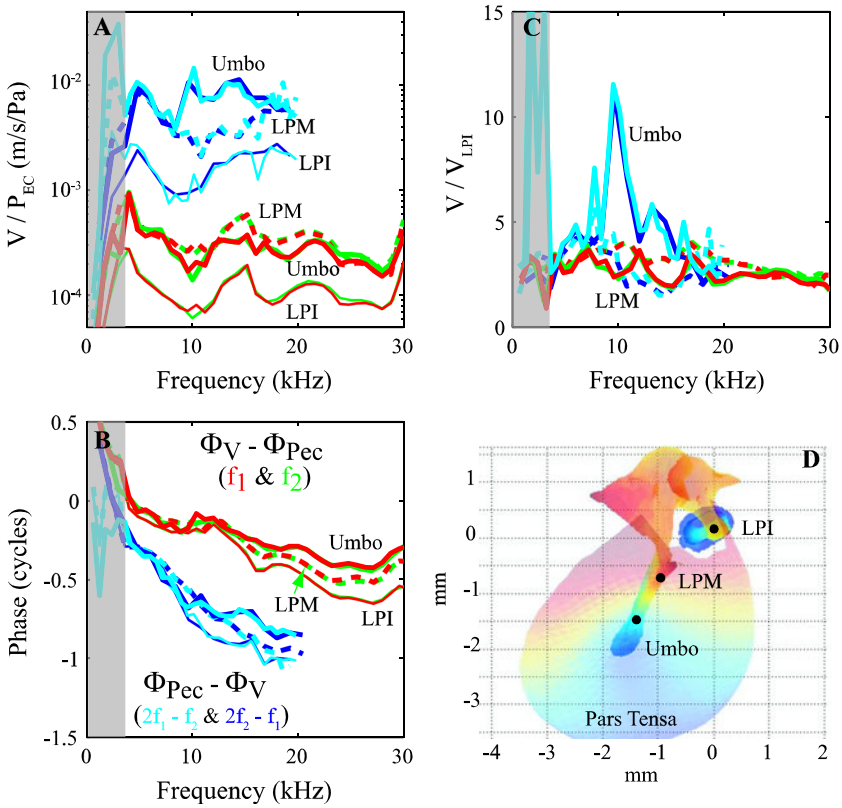

FIG. 9. Velocity along the manubrium from umbo to LPM. **A** Velocity/P_{EC}. **B** Phase difference in forward and reverse transmission. *Thin, dashed, and thick lines* represent LPI, LPM, and umbo, respectively. **C** Velocity/V_{LPI}. *Dashed and thick lines* represent LPM/LPI and umbo/LPI, respectively. (Experiment: 8 Apr. 2008, open-field sound configuration.). **D** Illustration of recording locations.

DISCUSSION

Previous studies of middle ear transmission based on measurements of EC and SV pressure showed that forward and reverse transmission were not inverses of one another. This is not a surprise, since the terminating load for forward transmission—the cochlea—is a very different load than the terminating load for reverse transmission—the air-filled EC (Ravicz et al. 1992, 1996). In our previous measurements in gerbil, there was 10–20 dB more loss in reverse transmission than gain in forward (Fig. 1 and Dong and Olson 2006). The major objective of the current study was to see whether differences in forward and reverse ossicular vibration occurred and if so whether they account for some of the extra loss in reverse transmission. Forward and reverse transmission were measured along the ossicular chain by comparing velocities to EC pressure at primary and DP frequencies. Ossicular measurements were made through the opening of the PF so that the measurement angle was approximately in the direction of stapes piston-like motion. Based on the results in Figures 3, 4, and 5, the forward versus reverse differences in global transmission (EC to SV) reviewed in Figure 1 are also present—and therefore accounted for—in the local transmission between EC and LPM and between EC and LPI. This leads to the hypothesis that along the ossicular chain, forward and reverse transmission will be similar. In order to explore this hypothesis, a detailed comparison along the ossicular chain was presented in Figures 6, 7, and 8. We found that the forward and reverse transmission ratios (LPM to LPI) were similar to within a few decibels except in the frequency region around 11–18 kHz, where the difference was ~6 dB—with the reverse LPM:LPI ratio less than the forward (Fig. 6). Thus, at most frequencies, the ossicular chain is not responsible for the forward versus reverse transmission difference between EC and SV pressure, but the ossicular chain does contribute to the difference at frequencies around 15 kHz.

In the more detailed look into ossicular motion of Figure 7, in the 14.4 kHz region, the motion of the ossicles was more erratic than at other frequencies, with a relatively large amount of wobble of the MI-joint. When we interpolated the ossicular chain motion in a co-linear system (Fig. 8), similarity between forward and reverse transmission was observed even at 14.4 kHz. The results support the idea that malleus and incus behave as rigid bodies in the region that was covered by the observation points, in both forward and reverse transmission.

Thus, our hypothesis above that motion along the ossicular chain in the gerbil middle ear—at least the motion component measured—is the same in forward and reverse transmission is broadly supported by the data. This similarity suggests that the motion of the ossicles is quite constrained by its attachments to the lateral wall (see Fig. 2B of de La Rochefoucauld et al.

2010) and the annular ligament of the stapes. Close to the EC, the forward:reverse similarity broke down; the umbo moved differently in reverse and forward transmission. The TM has relatively unconstrained and complex motion, and it is not surprising that the forward and reverse motions diverge at this point.

Umbo velocity and EC pressure were used to estimate the FTF and RTF in guinea pig by Dalhoff et al. (2011), and in general, the RTF was greater than the FTF, similar to our results. In addition, they observed a notch in the RTF; while the DPOAE was relatively smooth with frequency, the umbo velocity had a deep notch at ~8 kHz. The notch was attributed to an anti-resonance and analyzed with a lumped-element model of the middle ear. Our own single-point velocity measurements on the TM (not shown in the present paper) similarly showed peaks and valleys in the frequency response that were not seen in the DPOAE. Full-field holographic measurements (Rosowski et al. 2009; Tonndorf and Khanna 1972) are useful to describe and understand the complex patterns of TM motion, and such measurements were recently applied to reverse transmission (Cheng et al. 2011). The holographic measurements showed complex motion patterns in reverse transmission.

The principal finding of the present report is that, when viewed ~along the stapes piston-like direction, middle ear transmission along the ossicular chain from the LPM to the LPI was quite similar in forward and reverse directions. The 10–20-dB difference between forward and reverse transmission found when referencing to EC pressure does not occur along the ossicles, and therefore must be due to the differences in load impedances in the forward and reverse directions.

ACKNOWLEDGMENTS

We thank the three JARO reviewers, whose comments improved the quality of the paper. This research was supported by the NIDCD, the Emil Capita Fund, and the Fund for Scientific Research Flanders.

REFERENCES

AIBARA R, WELSH JT, PURIA S, GOODE RL (2001) Human middle-ear sound transfer function and cochlear input impedance. Hear Res 152:100–109

CHENG JT, HARRINGTON E, FURLONG C, ROSOWSKI JJ (2011) The tympanic membrane motion in forward and reverse middle-ear sound transmission. In: Proceedings of the 11th International Mechanics of Hearing Workshop, 16–22 July 2011, Williamstown, pp. 158–163

DALHOFF E, TURCANU D, GUMMER AW (2011) Forward and reverse transfer functions of the middle ear based on pressure and velocity DPOAEs with implications for differential hearing diagnosis. Hear Res 280:86–99

DANCER A, FRANKE R (1980) Intracochlear sound pressure measurements in guinea pigs. Hear Res 2:191–205

DE LA ROCHEFOUCAULD O, OLSON ES (2010) A sum of simple and complex motions on the eardrum and manubrium in gerbil. Hear Res 263:9–15

DE LA ROCHEFOUCAULD O, DECRAEMER WF, KHANNA SM, OLSON ES (2008) Simultaneous measurements of ossicular velocity and intracochlear pressure leading to the cochlear input impedance in gerbil. J Assoc Res Otolaryngol 9:161–177

DE LA ROCHEFOUCAULD O, KACHROO P, OLSON ES (2010) Ossicular motion related to middle ear transmission delay in gerbil. Hear Res 270(1–2):158–72

DECORY L, FRANKE RB, DANCER AL (1990) Measurement of middle ear transfer function in cat, chinchilla and guinea pig. In: Dallos P, Geisler CD, Matthews JW, Ruggero MA, Steele CR (eds) The mechanics and biophysics of hearing. Springer, Berlin, pp 270–277

DECRAEMER WF, DE LA ROCHEFOUCAULD O, DONG W, KHANNA SM, DIRCKX JJ, OLSON ES (2007) Scala vestibuli pressure and three-dimensional stapes velocity measured in direct succession in gerbil. J Acoust Soc Am 121:2774–2791

DECRAEMER WF, DE LA ROCHEFOUCAULD O, OLSON ES (2011) Measurement of the three-dimensional vibration motion of the ossicular chain in the living gerbil. In: Shera CA, Olson ES (eds) What fire is in mine ears: progress in auditory biomechanics. American Institute of Physics, Melville, pp 164–169

DONG W, OLSON ES (2005) Two-tone distortion in intracochlear pressure. J Acoust Soc Am 117:2999–3015

DONG W, OLSON ES (2006) Middle ear forward and reverse transmission in gerbil. J Neurophysiol 95:2951–2961

DONG W, OLSON ES (2008) Supporting evidence for reverse cochlear traveling waves. J Acoust Soc Am 123:222–240

KEEFE DH (2002) Spectral shapes of forward and reverse transfer functions between ear canal and cochlea estimated using DPOAE input/output functions. J Acoust Soc Am 111:249–260

KEEFE DH, ABDALA C (2007) Theory of forward and reverse middle-ear transmission applied to otoacoustic emissions in infant and adult ears. J Acoust Soc Am 121:978–993

KEMP DT (1978) Stimulated acoustic emissions from within the human auditory system. J Acoust Soc Am 64:1386–1391

MAGNAN P, AVAN P, DANCER A, SMURZYNSKI J, PROBST R (1997) Reverse middle-ear transfer function in the guinea pig measured with cubic difference tones. Hear Res 107:41–45

NAKAJIMA HH, OLSON ES, MOUNTAIN DC, HUBBARD AE (1994) Electrically evoked otoacoustic emissions from the apical turns of the gerbil cochlea. J Acoust Soc Am 96:786–794

NAKEJIMA HH, DONG W, OLSON ES, MERCHANT SN, RAVICZ ME, ROSOWSKI JJ (2008) Differential intracochlear sound pressure measurements in normal human temporal bones. J Assoc Res Otolaryngol 10:23–36

NEDZELNITSKY V (1980) Sound pressures in the basal turn of the cat cochlea. J Acoust Soc Am 68:1676–1689

OLSON ES (1998) Observing middle and inner ear mechanics with novel intracochlear pressure sensors. J Acoust Soc Am 103:3445–3463

OLSON ES (2001) Intracochlear pressure measurements related to cochlear tuning. J Acoust Soc Am 110:349–367

PURIA S (2003A) Measurements of human middle ear forward and reverse acoustics: implications for otoacoustic emissions. J Acoust Soc Am 113:2773–2789

PURIA S (2003) Middle-ear two-port measurements in human cadaveric temporal bones: comparison with models. Proceedings of the 3rd Symposium on Middle Ear Mechanics in Research and Otology, Japan, World Scientific, pp. 43–50

Puria S, Rosowski JJ, Peake WT (1993) MIddle ear pressure gain in humans: preliminary results. World Scientific, Singapore

Puria S, Peake WT, Rosowski JJ (1997) Sound-pressure measurements in the cochlear vestibule of human-cadaver ears. J Acoust Soc Am 101:2754–2770

Ravicz ME, Rosowski JJ, Viogt HF (1992) Sound-power collection by the auditory periphery of the Mongolian gerbil *Meriones unguiculatus*. I: Middle-ear input impedance. J Acoust Soc Am 92(1):157–77

Ravicz ME, Rosowski JJ, Viogt HF (1996) Sound-power collection by the auditory periphery of the Mongolian gerbil *Meriones unguiculatus*. II: External-ear radiation impedance and power collection. J Acoust Soc Am 99(5):3044–63

Ravicz ME, Cooper NP, Rosowski JJ (2008) Gerbil middle-ear sound transmission from 100 Hz to 60 kHz. J Acoust Soc Am 124:363–380

Rosowski JJ, Cheng JT, Ravicz ME, Hulli N, Hernandez-Montes M, Harrington E, Furlong C (2009) Computer-assisted time-averaged holograms of the motion of the surface of the mammalian tympanic membrane with sound stimuli of 0.4-25 kHz. Hear Res 253:83–96

Slama MC, Ravicz ME, Rosowski JJ (2010) Middle ear function and cochlear input impedance in chinchilla. J Acoust Soc Am 127:1397–1410

Teoh SW, Flandermeyer DT, Rosowski JJ (1997) Effects of pars flaccida on sound conduction in ears of Mongolian gerbil: acoustic and anatomical measurements. Hear Res 106:39–65

Tonndorf J, Khanna SM (1972) Tympanic-membrane vibrations in human cadaver ears studied by time-averaged holography. J Acoust Soc Am 52:1221–1233

Voss SE, Shera CA (2004) Simultaneous measurement of middle-ear input impedance and forward/reverse transmission in cat. J Acoust Soc Am 116:2187–2198

Withnell RH, Kirk DL, Yates GK (1998) Otoacoustic emissions measured with a physically open recording system. J Acoust Soc Am 104:350–355